Ultrasonic-assisted Dunlop method for natural rubber latex foam production: Effects of irradiation time on morphology and physico-mechanical properties of the foam

Benjatham Sukkaneewat [a,b], Songkot Utara [a,b,*]

[a] Functional Materials and Composites Research Group, Faculty of Science, Udon Thani Rajabhat University, Udon Thani 41000, Thailand
[b] Division of Chemistry, Faculty of Science, Udon Thani Rajabhat University, Udon Thani 41000, Thailand

ARTICLE INFO

ABSTRACT

An ultrasonic-assisted technique was first introduced for the production of natural rubber latex foam (NRLF). The flexible elastomeric foam was formed by a liquid–solid state transformation in an aqueous media. The aim of the current research was to provide a novel strategy for fabricating NRLF using ultrasonication and the Dunlop method, as well as to simultaneously utilize irradiation events to achieve the desired foam properties. NRLFs were exposed to ultrasonication at 25 kHz at the beginning of the gelling process. The effects of irradiation times of 0, 1, 3, 5 and 7 min on the morphology, foaming behaviors, physical properties and mechanical performance of NRLFs were investigated. The results revealed that using ultrasonic irradiation, unfoamed regions and a bimodal structure, which seem to be microstructural defects in conventional NRLF, could be completely eliminated. However, excessive irradiation times of 5 min and longer appeared to affect the physico-mechanical properties of the foams in terms of transient cavitation and the unfavorable physicochemical effects of ultrasonic vibrations. As a result, the optimal ultrasonic irradiation time was found to be 3 min. Using this irradiation duration, a foam with the suitable microcellular structure achieved the most desirable properties, such as its expansion ratio (7-fold increase), foam porosity (85.7%), compression recoverability (98.7%), and tensile strength (307.3 kPa). Moreover, the foam still maintained its characteristic soft nature (hardness less than 100 N) with an indentation hardness of 71.9 N. Therefore, ultrasonic treatment introduced to the conventional Dunlop method is a potentially feasible technique since it improves the morphology and the physico-mechanical properties of NRLFs.

1. Introduction

Flexible polymeric foams have been utilized in a variety of products owing to their advantages of light weight, buoyancy, supporting properties, sound absorption, impact insulator and resin usage reduction [1–3]. The foams are generally produced from synthetic and natural polymers. Synthetic polymers and elastomers, namely poly(ethylene-co-vinyl acetate) (PEVA), ethylene-propylene-diene elastomer (EPDM), styrene-butadiene rubber (SBR) and polyurethane (PUR), are employed to make commercially available elastomer-based foams [4,5]. However, many synthetic polymers are not sustainable resources and generate pollutants because they are not biodegradable. One of the best ways to mitigate pollution is to use biomaterials. NRLF is fabricated using natural rubber (NR) latex, which is a bioderived material and a renewable resource. The NR matrix contains 94% *cis-1,4*-polyisoprene and 6% non-rubber composition [6]. Apart from the high elasticity of NR's main component, its non-rubber constituents provide some unique characteristics, e.g., high tensile strength, tear strength, and toughness [7]. NRLFs are also recognized as sponge and expanded rubbers. They are cross-linked specimens with air bubbles inside the polymer matrix formed *via* a liquid–solid state transformation of NR latex [8,9]. These bio-based foams undergo their foaming processes through a three-phase colloidal system, involving rubber particles, gas bubbles and an aqueous phase. The microstructures of NRLF can be divided into three categories, completely interconnected, partly interconnected and non-interconnected cellular structures. The foam properties, e.g.,

flexibility, density, indentation hardness, compression set, thermal insulation, mechanical properties and energy absorption, also depend on these cellular architectures [8]. Therefore, to obtain desired properties, several studies have attempted to control the microstructure of rubber foams using various techniques, such as a microbubbling technique [10], a microwave processing technique [11], electron beam irradiation [12] and a filler-assisted technique [13,14]. However, morphological control in thermoset foams (rubber foams) is still a challenge and appears more complex than that in thermoplastic foams since they are comprised of several phases and must be nearly simultaneously foamed and vulcanized [12,14].

The Dunlop and Talalay processes are two well-known NRLF production methods. The Talalay method provides softer NRLFs with greater flexibility than the Dunlop method [10]. However, the Dunlop method is commonly used as it is convenient, dependable, cost-effective, organic solvent-free and more energy-efficient [15,16]. In the Dunlop method, NR latex is first compounded with vulcanizing and foaming agents and whipped into a froth. The liquid foam is then mixed with a delayed-action gelation reagent, i.e., sodium fluorosilicate (NaFS), and poured into a mold to gel and become a solid foam before being vulcanized in an oven. After vulcanization, the foam is cleaned and moisture eliminated from the finished product [16]. To the best of our knowledge, the Dunlop method does not involve any technical step for controlling the microstructure quality of the foam, even though the microcellular structure can be an important parameter that greatly influences physico-mechanical properties of rubber foams [8,10–12]. In other words, NRLFs prepared by the Dunlop method still require some production techniques that allow manipulation their cellular orientation.

Ultrasonic irradiation is an effective approach to generate numerous froths in fluid. Cavitation creates extreme localized conditions, such as hot spots (high temperature and pressure), as well as other events, namely acoustic streaming, rapid mixing, micro jetting and interparticle collisions in slurries [17,18]. Several studies have shown that ultrasonic irradiation can be applied to alter the foaming behaviors of various polymeric foam types. Ultrasonic oscillations can promote cell nucleation, which leads to more uniform cell structures in both melted and solid polymer foams [19–21]. It was also used to aid in melt extrusion foaming of polymer foams, resulting in increased cell density [22,23]. In PUR foam formation, blowing and solidification reactions occur simultaneously when the starting chemicals react with each other. Ultrasonication changes the volume and distribution of pores in the direction parallel to foam rise using localized physical and chemical processes [24]. Ultrasonic-assisted preparation has received great interest for solid-state foaming processes. Polystyrene (PS), poly(lactic acid) (PLA) and acrylonitrile-butadiene rubber (NBR) foams, fabricated using a CO_2-saturated method, exhibited enhanced foaming due to ultrasonic irradiation. By applying ultrasonic waves at the onset of foaming, the polymer foams had a significantly increased expansion ratio and cell density [25–27]. Recently, ultrasonication was done to prepare grafted polymer foams derived from polyvinyl alcohol/phytic acid (PVA/PA). Aside from their foam-aided performance, sonochemical effects generate chemical species that induce establishment of phosphonate and ether bonds between the PVA chains and PA, leading to successful grafting of the PVA/PA foam [28].

Ultrasonic irradiation has been used for improving the microstructure and properties of thermoplastic and rigid thermoset foams in both solid- and melted-state forms. To date, the use of ultrasonic irradiation with a considerably flexible thermoset foam formed *via* liquid–solid state transformation in an aqueous media (or the NRLF) as well as incorporation of an ultrasonication technique with the Dunlop method for NRLF production have never before been reported. Additionally, findings from the previous work of our research group revealed that ultrasonic vibrations can generate numerous tiny bubbles in NR latex (a templating agent) during the synthesis of nano–hydroxyapatite particles [29]. Therefore, this is the first report of using an ultrasonic-assisted

technique to tune the microstructure of NRLF. The effects of ultrasonication period on the morphology, physical properties and mechanical performance of NRLF were investigated here. The relationships among those properties are discussed. Finally, the possible physicochemical impacts of ultrasonication at the molecular level of NRLF are also proposed.

2. Materials and methods

2.1. NRLF materials

NR latex with 60 wt% dry rubber and high ammonia content, potassium oleate (KO), sulfur (S), zinc diethyldithiocarbamate (ZDEC), zinc 2-mercaptobenzothiazole (ZMBT), Wingstay®-L, Melaniline (MN), zinc oxide (ZnO) and sodium fluorosilicate (NaFS) were acquired from the Rubber Research Institute of the Rubber Authority of Thailand (RAOT), Bangkok, Thailand. All chemicals were of commercial grade and used as an aqueous dispersion form with the total solid levels given in Table 1. Distilled water was employed throughout the foam preparation.

2.2. Preparation of NRLF by the conventional Dunlop method

NRLFs were fabricated using the chemical proportions given in Table 1. NR latex was filtered and mechanically agitated at 80 rpm for 35 min to liberate dissolved ammonia prior to foam preparation. The Dunlop method consists of four processes, namely compounding, foaming, gelling and vulcanization [8]. In the first process, NR latex was blended with KO, S, ZDEC, ZMBT and Wingstay®-L using mechanical stirring at 80 rpm for 60 min. After that, the mixture was beaten at 800 rpm for 3 min using a stand mixer resulting in a five-fold increase in its volume during the foaming process. This foam is referred to as the liquid NRLF. Then, the speed of the mixer was reduced to 160 rpm, while the liquid NRLF was continuously beaten for 30 sec so that it possessed a fine cellular structure. This mild beating was extended for 1 min, while ZnO, MN and NaFS (gelling reagents) were consecutively added to the liquid NRLF. Then, the non-gelled NRLF was immediately poured into a mold to begin the gelling process. The molded NRLF was left at room temperature for 7 min (the solidification time) to completely form a solid foam. Finally, NRLF was vulcanized at 100 °C for 90 min in an oven (UF110, Memmert). The non-reactive reagents were removed by washing the solid foam with distilled water followed by drying at 70 °C for 24 h. The gel time, related to the interval in which the liquid foam transforms to gel during the gelling process, was recorded for all NRLF preparations. Gel time measurements were conducted in glass cups (600 mL) and performed using ASTM D 7487–18 methodology with slight modifications from earlier reports [5,30,31]. Although this method is developed for PU molded foam, the physical process of waiting for the gel appearance between PU molded foam and NRLF is somewhat similar. After pouring the liquid NRLF into the mold, a depressor rod was used to touch the surface of the foam periodically until persistent rubber strings could be observed and pulled at least 40 mm out from the surface

Table 1
Chemical formulation for the NRLF preparation.

Chemicals	Total solid amount (%)	Dry weight in recipe (phr[a])
NR latex	60%	100
KO	10%	1.5
S	50%	2.5
ZDEC	50%	1.0
ZMBT	50%	1.0
Wingstay®-L	50%	1.0
ZnO	50%	3.0
MN	33%	1.0
NaFS	12.5%	0.45

[a] phr is the ratio unit of weight part of chemicals to 100 wt parts of rubber

of the foam. This time was recorded using a digital stopwatch in three repeated tests and reported as the average gel time of non-irradiated NRLF (4.36 ± 0.03 min).

2.3. Preparation of NRLF by the ultrasonic-assisted Dunlop method

The same formula and fabrication processes described previously were also conducted for ultrasonic-assisted preparation of NRLF, except for the gelling process. Fig. 1 shows the experimental procedures for NRLF preparation using the ultrasonic-assisted Dunlop method. An ultrasonic transducer (diameter of 5.0 cm) in conjunction with a water bath, served as an ultrasonic reactor in this work. Ultrasonic irradiation with frequency of 25 kHz was introduced to NRLFs at the start of the gelling process, when the liquid–solid state transformation of NRLFs gradually occurred. After foaming (beating), mixing gelling reagents into the foams and pouring the foams into a mold, non-gelled liquid NRLFs were quickly irradiated by submerging them in the ultrasonic reactor, as presented in the inset of Fig. 1. For all irradiated samples, the temperature and distance between the ultrasonic transducer and the mold were kept at 40 °C and 1.0 cm, respectively. The irradiation times were varied at 1, 3, 5 and 7 min. The solidification time of all irradiated foams was fixed at 7 min to ensure that both irradiated and non-–irradiated foams had equal solidification time. After removing the irradiated foams from the ultrasonic reactor, the foams irradiated for 1, 3 and 5 min were rested at room temperature for 6, 4 and 2 min,

respectively, while the foam irradiated for 7 min was immediately transferred to the oven at the vulcanization temperature. The gel times of NRLFs prepared by the ultrasonic-assisted Dunlop method with irradiation times ranging from 1 to 7 min were recorded as 4.32 ± 0.04, 4.37 ± 0.04, 4.36 ± 0.02 and 4.35 ± 0.04 min, respectively. Finally, washing and drying processes were performed under the same conditions as those of the conventional Dunlop method.

2.4. Characterizations

2.4.1. Morphological properties

The microcellular structures of NRLFs were studied using a Hitachi S-3000 N scanning electron microscope (SEM) operating at 5 kV. Dried foams were submersed in liquid N_2, fractured and vacuum-coated with gold prior to SEM investigation. Average cell diameters and cell wall thicknesses were evaluated using Image J software Version 1.53 k. Cell size distribution was quantitatively examined by sampling at least 100 cells of each foam. Cell density, N (cells/cm³), was calculated as Eq. (1):

$$N = \frac{6}{\pi d^3}\left(\frac{\rho_r}{\rho_f} - 1\right) \tag{1}$$

where d, ρ_f and ρ_r are the average cell diameter, the density of NRLF and the density of solid NR (0.93 g/cm³), respectively.
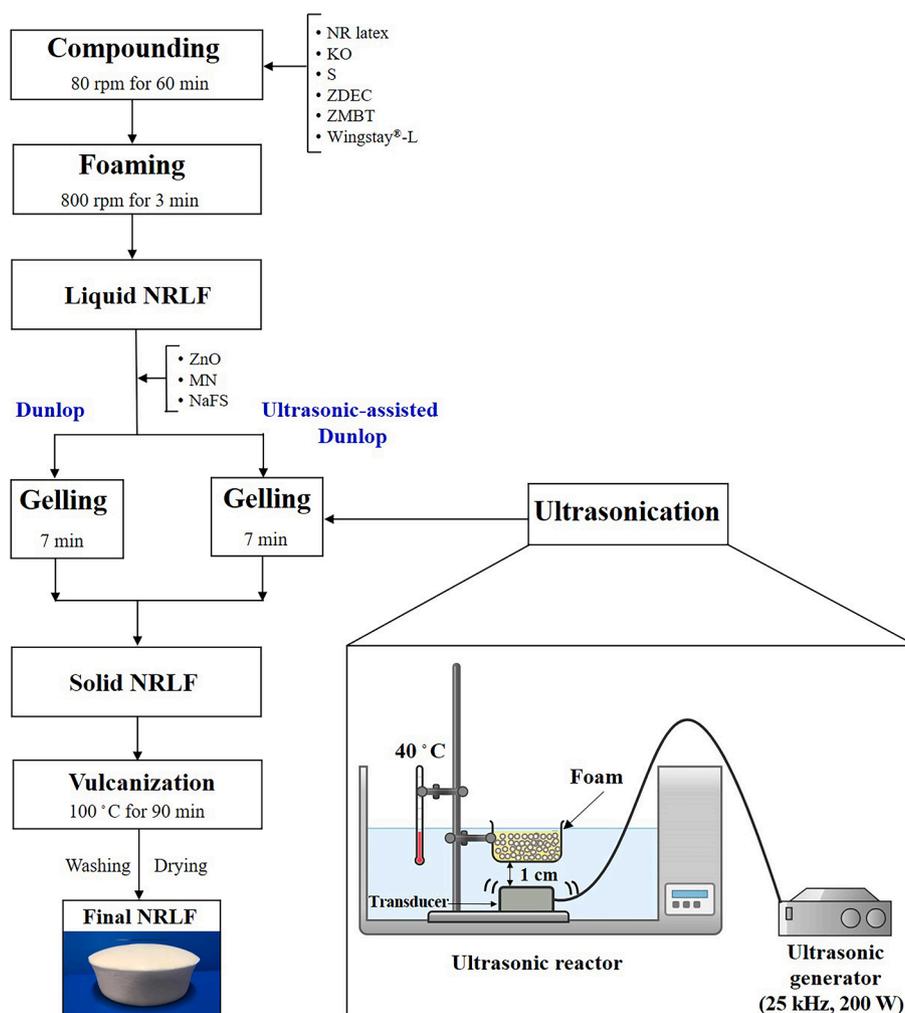
Fig. 1. Experimental procedures for NRLF production using the conventional Dunlop and the ultrasonic-assisted Dunlop methods. The inset presents a schematic representation of the ultrasonic reactor.

2.4.2. Physical properties

The average density measurements of NRLF were conducted from at least five foam specimens following ISO 845. Foam cubes with dimensions of $50 \times 50 \times 50$ mm^3 were cut using an electric knife (Kenwood KN-650), whose dual blades were thin-coated with a very small amount of lubricant before cutting. To obtain precise shapes, cutting lines were marked on the foam specimens, both parallel and perpendicular to the cutting direction. Foam dust was blown off from the surface of the foam using a dryer before weighing the specimens. The dimensions of each specimen side, used for calculating the corresponding volume, were measured using the Vernier caliper. The mass of foam specimens (m_f) was divided by their corresponding volume (V_f) to obtain the density of NRLF as shown in Eq. (2):

$$\rho_f = \frac{m_f}{V_f} \tag{2}$$

Indentation hardness tests were investigated according to ISO 2439 (Method A) using a foam compression machine (IDM-F0013, Australia). The NRLF specimen was placed on a supporting surface that had several 6 mm diameter vent holes to permit gas liberation from underneath the foam specimen during compression. During testing, the foam specimen was compressed by an indentor using a deformation rate of 100 mm/min. The indentation hardness was determined after the foam height was reduced to 40% for 30 sec.

A compression set tests were carried out according to ISO 1856 (Method B) using a compression set tester (JIS-A5756, Japan). NRLF test pieces with a thickness of 25 mm were put between the tester's metal plates and compressed to 50% of their initial thickness for 72 h at 23 °C. Then, the test pieces were removed from the instrument and rested for 30 min to allow them to return to their original shapes. The permanent compression set (*CS*) as a percentage was computed using Eq. (3):

$$CS = \frac{T_i - T_f}{T_i} \times 100 \tag{3}$$

where T_i and T_f are the initial and final foam thicknesses, respectively.

2.4.3. Foaming behaviors

Foaming behaviors of NRLF were studied in terms of their expansion ratio (*ER*) and foam porosity (V_f). An expansion ratio represents the ability of cellular materials to increase their unit volume during foam formation. This value was obtained from the ratio of solid NR density to NRLF density as presented in Eq. (4):

$$ER = \frac{\rho_r}{\rho_f} \tag{4}$$

Porosity, the percentage of void volume fraction inside the foam structures, was calculated using Eq. (5):

$$V_f = \left(1 - \frac{\rho_f}{\rho_r}\right) \times 100 \tag{5}$$

2.4.4. Mechanical properties

Tensile tests were conducted following ISO 1798 to characterize the mechanical properties of the flexible elastomeric foams. NRLF specimens were prepared using die-cutting to have the specified dimensions (Type 1A) prescribed by the standard method. The tests were performed on an INSTRON universal testing machine (5567A, USA) with a crosshead speed of 50 cm/min. Ultimate tensile strength, elongation at break and moduli at 100, 300 and 500% strain were determined from the resulting stress–strain curves.

3. Results and discussion

3.1. Morphological properties

Fig. 2 presents microcellular structures of NRLF with and without ultrasonication. Non–irradiated foam (Fig. 2(a)) had non-uniform cell structures. The bimodal structure, which consisted of large foam cells surrounding by the groups of small foam cells, and the unfoamed region, which is indicated by the red arrows in Fig. 2(a) and Fig. S1, could be observed. Very large cells indicate that adjacent foam cells coalesced during the liquid–solid state transformation. The cell coalescence and lack of cell homogeneity can result in structural collapse, affecting both the physical and mechanical properties of cellular materials [11]. This poor morphology was reported in other studies of NRLF produced using the Dunlop method [10,16]. When foaming processes of polymeric cellular materials were carried out in a multi-phase system, cell nucleation is nonuniform [26].

In contrast, the morphology of irradiated foams was significantly changed with the introduction of ultrasonic irradiation (Fig. 2(b)-(e)). The unfoamed regions disappeared, while the bimodal structure was gradually minimized in all samples. Cellular uniformity greatly improved with longer irradiation times owing to the increased number of finer foam cells. NRLF with an irradiation time of 7 min showed the finest cellular structure, which can be attributed to the cell nucleating effect induced by the acoustic vibrations (Fig. 2(e)). According to the literature, the microbubble implosion of ultrasound wave in an aqueous media can generate tiny cell nuclei having much smaller initial radii, which can grow to become more uniform and finer foam cells [17,21,32].

Quantitative distribution curves are plotted against cell sizes as shown beside each foam morphology in Fig. 2. Non-irradiated foam showed a wide distribution curve with a broad range of cell sizes of 119.6–733.2 μm owing to its bimodal structure. The cell size distribution of the irradiated foams became more uniform after 1 min of irradiation. However, large cell sizes, greater than 400 μm, were still visible. Narrower curves of cell size distribution were clearly obtained with irradiation times from 3 to 7 min (Fig. 2(c)-(e)). The size distribution curves gradually shifted to zones of smaller cell sizes, 65.3 – 294.6 μm, as the irradiation time reached 7 min. Examination of morphology and cell size distribution revealed that the uniformity of microcellular structures of NRLF is improved with applied ultrasonication and longer irradiation times. When a large number of finer foam cells occur *via* the nucleating effect of ultrasonic vibrations, the solidified NRLFs had more ordered cellular structures. This result is in accordance with that reported by Gandhi et al. [21]. They found that as irradiation time increased, the morphology of acrylonitrile–butadiene–styrene foams became more homogeneous with smaller cells.

In order to confirm the role of ultrasonication in improvement of the morphological properties of NRLFs, the average cell diameters and cell densities of NRLFs at various irradiation times were studied (Fig. 3). The non-irradiated NRLF showed the largest average cell diameter of 262.7 $\pm$ 130.8 μm. As expected, the foams with longer irradiation times of 1, 3, 5 and 7 min exhibited decreased average cell diameters of 200.6 $\pm$ 66.4, 186.8 $\pm$ 57.9, 166.8 $\pm$ 58.2 and 151.3 $\pm$ 51.1 μm, respectively. These results confirm that foam cells developed from smaller nuclei have smaller cell diameters after exposure to ultrasonic irradiation for prolonged periods of time. The standard deviation (SD) included with the average cell diameter is strongly influenced by the variation of foam cell diameter. NRLFs are foamed through the three-phase colloidal system with no specific microstructure-controlling step. Thus, it seems difficult to regulate their cell diameter variation. For non-irradiated foam, the non-uniform morphology and bimodal structure cause this foam to have large cell diameter differences as shown by the board size distribution curve, increasing the maximum SD values. The greater uniformity of smaller cell diameters helps to decrease the SD values in the case of the irradiated foams. Therefore, applied ultrasonic waves can act as a
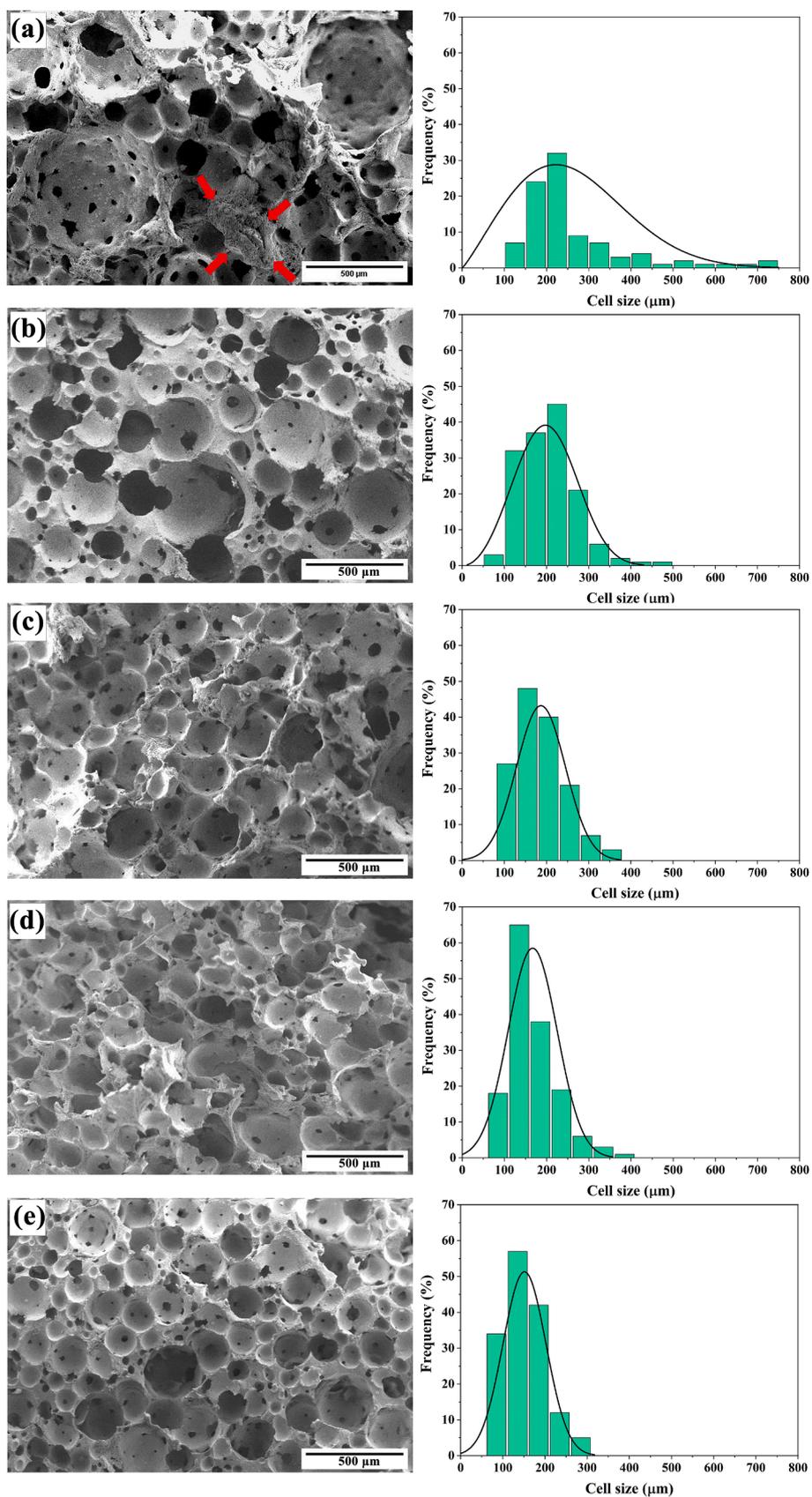
Fig. 2. SEM micrographs and cell size distribution curves of NRLFs at various ultrasonic irradiation times: (a) 0 min, (b) 1 min, (c) 3 min, (d) 5 min, and (e) 7 min.
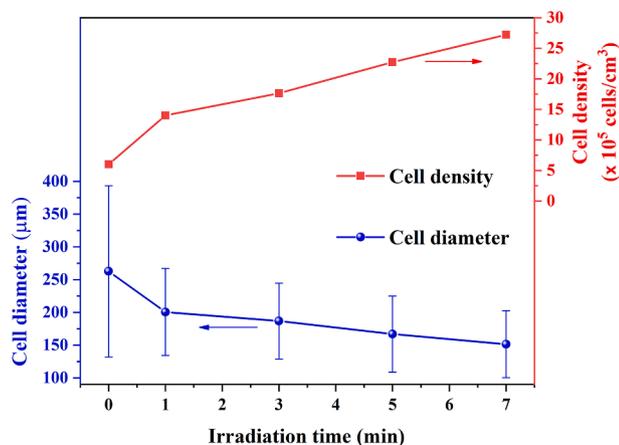
Fig. 3. Average cell diameter and cell density of NRLFs at various ultrasonic irradiation times.

homogeneous bubble nucleation process for flexible elastomeric foams fabricated using the Dunlop method.

It is notable that the average cell diameters of NRLFs decreased sharply with irradiation times from 0 to 3 min, whereas this decrease was more gradational with irradiation times from 3 to 7 min. Gel time and viscosity increase during gelling process seemed to be the related factors that determine the cell diameter of NRLF. Therefore, to explain this observation, we considered the relationship of both factors with the ultrasonic working performance. According to the experimental data, the gel times of irradiated foams were nearly identical to that of the non–irradiated foam, ranging from 4.32 ± 0.04 to 4.37 ± 0.04 min. This result indicates that there is no relationship between the gel time of the rubber foams and the ultrasonic works. In the other words, it is clear that the introduction of ultrasonication to the Dunlop method does not affect the gelation and the processing time of the foam production. Another factor is viscosity buildup during liquid–solid state transformation. Before gel formation, the viscosity of the foam system slightly increases, and the NRLFs with irradiation times of 0 to 3 min are liquid foams with lower viscosity. At this stage, the foam cells are more easily nucleated and dispersed by ultrasonic irradiation, resulting in a notable reduction in the average cell diameters. However, after this interval, highly viscous liquid and elastic solid-like foams are formed with irradiation for 3–5 min (during gelation) and 5–7 min (after gelation), respectively. A large viscosity increase during this phase transition promotes viscoelastic stress in the polymeric matrix, which may retard the ultrasonic working performance for microcellular manipulating *via* limiting the stretching motion of foam cells to alter their diameters.

In the case of cell density (Fig. 3), there was an inverse relationship with the average cell diameter. Longer irradiation times resulted in higher cell density values. An irradiation time of 7 min resulted in a 4.5–fold increase of cell density to 27.2×10^5 cells per cm^3 compared to 6.0×10^5 cells per cm^3 for non–irradiated foam. This suggests creation of smaller foam cells increased cell numbers per unit volume. Therefore, ultrasonic irradiation can inhibit foam cell coalescence, which occurs easily for the liquid-state foam and results in large cell sizes with low cell density of the final foam.

Another significant influence of ultrasonic irradiation on morphological properties of the flexible elastomeric foam is the wall thinning effect. As observed from the SEM micrographs, foam cell boundaries appeared thinner with increased irradiation time. The cell wall thickness of non-irradiated NRLF was 29.1 ± 21.3 µm. Whereas, cell walls of irradiated foams were thinned to 21.6 ± 17.3, 14.2 ± 6.2, 10.6 ± 6.1 and 9.1 ± 3.7 µm by applying irradiation for 1, 3, 5, and 7 min, respectively. Turbulent convection from the ultrasonic field creates stress that can accelerate wall thinning of foam cells during foam expansion [33].

3.2. Foaming behaviors

Fig. 4 presents plots of the expansion ratio and porosity of the foams versus irradiation time. It was found that these parameters had similar trends. Both the expansion ratio and porosity increased as irradiation time was advanced from 0 to 3 min. Then, they decreased as irradiation time was prolonged further. The maximum expansion ratio about 7-fold increase and the highest foam porosity of 85.7% were achieved at the irradiation time of 3 min. Conversely, the foam samples irradiated for 5 and 7 min showed not only decreased expansion ratios and porosity, but also worse values than those of the non-irradiated foam. These findings indicated that while longer irradiation time improved the morphological properties of NRLF, excessive irradiation for periods of 5 and 7 min impaired some foaming behaviors.

Optimal irradiation time provides stable cavitation, while immoderate irradiation time results in transient cavitation [32]. The applied ultrasonic field generates both stable and transient cavitation events that cause foam nuclei to alternate their bubble dynamics during cell growth and expansion. When foam nuclei are irradiated in stable cavitation, they oscillate with the resonance of the ultrasonic wave without structural deformation. The nuclei are forced to expand their volume due to the sinusoidal nature of ultrasound during this time, resulting in an increased expansion ratio with irradiation times of 0 to 3 min. However, when transient cavitation occurs as a result of an excessive treatment, foam cells become overexcited and are unable to oscillate with the ultrasonic wave resonance. Thus, the cell walls cannot be stabilized causing collapse of foam cells [32,34]. Furthermore, Wang et al. explained that when the cell density was too high, foam growth was restricted, leading to a lower foam expansion ratio [23]. Several researchers reported that transient cavitation caused not only foam collapse, but also cell rupture in rigid polymer foams, such as those of PUR [32], PLA [35] and PS [36]. The effects of transient cavitation on the foaming behaviors of flexible elastomeric foams in aqueous media have never been reported. In the current study, the foam rupture of irradiated NRLFs was not found. This might be related to the ultra-high elasticity of natural rubber matrix.

A strong relationship between expansion ratio and foam porosity was observed, as the latter depends on the volume fraction of voids inside a cellular structure. When air bubbles, which act as nuclei of foam cells, have a greater ability to grow with the positive effects of ultrasonic stimulation, the volume of air bubbles in rubber matrix expands. This causes the volume fraction of voids in the cellular structure to increase, resulting in higher porosity and vice versa [23]. Therefore, the highest porosity can be obtained with the greatest expansion ratio. An increased expansion ratio is required for polymer foam production since it provides lightweight final products and reduces the amount of polymer
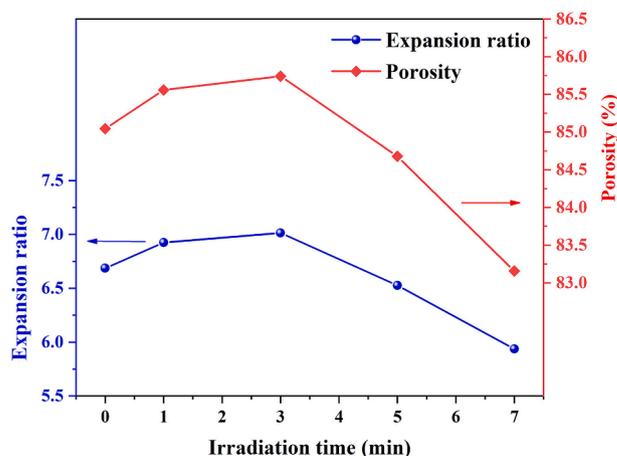
Fig. 4. Expansion ratio and porosity of NRLFs at various ultrasonic irradiation times.

resin used [26]. An increased expansion ratio can be accomplished by elevating the foaming temperature [13,26]. Nevertheless, the results of the current work reveal that higher expansion ratio can be obtained by applying the dissipated energy of ultrasonic waves at an optimal irradiation time without the addition of external heat. Therefore, it may be deduced that ultrasonic irradiation also serves as an endothermic dissipation process for NRLF preparation.

The appearance of demolded foams, which resulted from different foaming behaviors, was captured (Fig. 5). The red lines over the foam surfaces were marked at the same level and used to indicate the foaming ability of NRLFs. The non-irradiated foam clearly demonstrated shrinkage of the top surface, which can be attributed to cell coalescence, unfoamed regions, and non-uniform cell sizes. However, the foams irradiated for 1 and 3 min present fuller curves on their top surfaces, implying higher and more stabilized foam expansion. For the foams irradiated for 5 and 7 min, their top surfaces became slightly flat owing to lower foam expansion and slight collapse of foam cells, as previously discussed.

3.3. Physical properties

Density and indentation hardness are important physical parameters for NRLFs because density dictates the weight of the final products for lightweight design applications. Additionally, indentation hardness impacts the load-bearing capacity of the foam, especially for body-supporting applications [11,37]. Fig. 6 presents the foam density and indentation hardness with varying irradiation times. In comparison to a non-irradiated foam, the density of irradiated foams reduced initially until irradiation times reached 3 min. Then, it increased with longer irradiation times of 5 and 7 min. This behavior may be attributed to the dissimilar effects of the acoustic fields in various foam states. Since NRLFs remain in the liquid state after 1 and 3 min of irradiation, ultrasonic vibration can act as an endothermic dissipation process to improve both their expansion ratio and foam porosity. As a result, the volume of the foams increases in inverse proportion to density, resulting in decreased foam density. Moreover, ultrasound probably reduces the foam density in other ways. First, ultrasonic irradiation performs dynamic agitation to increase the limit of gas solubility in a liquid polymeric foam. Second, dissipated ultrasonic energy enhances the permeability of foam cell walls through a wall thinning effect and simultaneously increases the gas diffusion coefficient. These promote gas diffusion into foam nuclei [32,34]. However, when the foams transform to the solid-state foams (irradiation times of 5–7 min), it is more difficult to diffuse gas into a solid polymer resin. Excessive irradiation causes thermodynamic instability in a solid polymer/gas system and might promote massive gas loss, which leads to foam collapse, lower
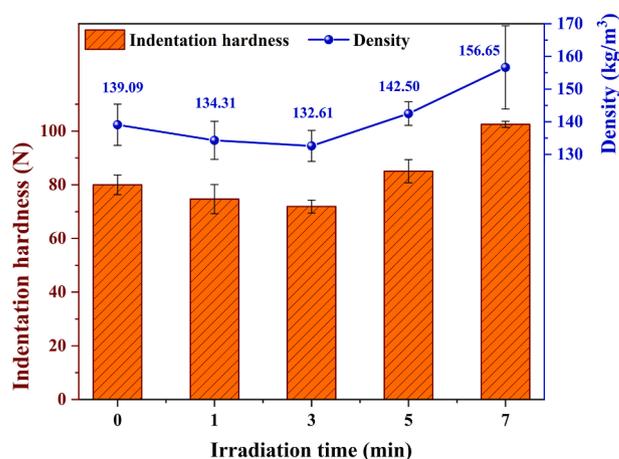
Fig. 6. Density and indentation hardness of NRLFs as a function of ultrasonic irradiation times.

expansion ratios and increased density [21].

Indentation hardness, the compressive stress used for indenting a compressive strain over a specific area, is more commonly used to evaluate the load-bearing capacity of NRLF than the compressive strength. This is because it provides information about the stress at a localized area rather than over a wider area, which is more useful information for flexible foams [8]. Foam density, porosity and cell size compete with each other to determine the indentation hardness of foams [38,39]. Fig. 6 presents how indentation hardness decreases as the foam density is reduced and vice versa. An increased expansion ratio reduces foam density, which leads to a softening effect [8]. Additionally, it is possible that the foams with lower density appear softer because they possess less compact interiors as well as less polymer mass. As such, they require lower indenting loads to deform their cellular structures. Cell diameter and foam porosity also impact indentation hardness. Tang et al. suggested that foam hardness increased with decreasing cell diameter and percentage of porosity, but it was more dependent on percentage of porosity [39]. In the current study, foam porosity directly impacts indentation hardness to a greater degree than the cell diameter effect. This was clearly observed in the case of NRLFs with irradiation times ranging from 0 to 3 min. The indentation hardness of those foams consistently decreased with longer irradiation times owing to their increased percentage of porosity, even though their cell diameters decreased. The indentation hardness of foams with irradiation durations between 3 and 7 min increased again with decreases of both cell diameter and percentage of porosity. When the percentage of porosity
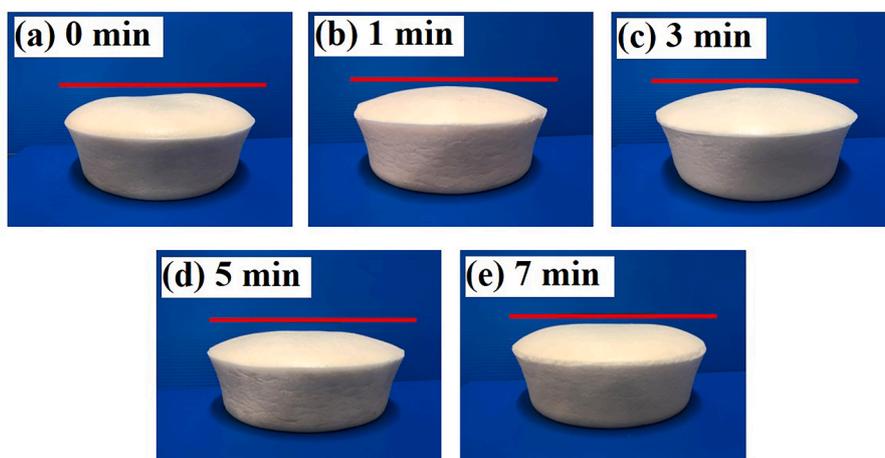
Fig. 5. Appearance of NRLFs after demolding at various ultrasonic irradiation times.

increases, the void areas which are not occupied by the solid rubber also increase. This causes the foams to have higher compressibility degree under the indentation force, resulting in lower indentation hardness and vice versa. According to the standard classification (ISO 2439), foam materials with hardness values lower than 100 N can be classified as soft foams [10]. Hence, NRLFs under the ultrasonic dissipation process with irradiation time less than 5 min can be classified as soft foams. They may have a potential for further development as body-supporting materials.

Apart from indentation hardness, the compression set, permanent deformation of material under long-term compression, and foam recoverability were also evaluated as factors that affect the shelf life of NRLF products. Generally, better foam recoverability results from smaller permanent compression set [40]. Fig. 7(a) and (b) demonstrate compression set and foam recoverability, respectively, as a function of irradiation times. Non-irradiated foam had a compression set of 2.9 ± 0.6% and recovery percentage of 97.1 ± 0.6%, which are typical values for conventional NRLF produced using the Dunlop method [8]. Foams with a lower compression set and higher recoverability were achieved by introducing ultrasonication and increasing irradiation times to 1 and 3 min. A foam with a suitable irradiation time of 3 min demonstrated a minimal permanent compression set of 1.3 ± 0.4% and the highest ability to recover its former shape, more than 98%. Elastomers, especially natural rubber, possess good resilience and inherent elasticity. Their permanent compression deformation can be considerably

improved by transforming them into foam materials through incorporation of gas bubbles in a rubber matrix [39]. Herein, the quality of foam microstructure seems to be a key parameter affecting compression set and foam recoverability [13,39,40]. Non-irradiated foam exhibited poor morphology. It comprised of unfoamed regions (Fig. S1) and lacked uniformity of cellular structures Fig. 2(a). This led to its loss of the ability to recover its initial shape after the release of confining stress, and subsequent higher permanent compression set and lower foam recovery [10]. For the irradiated foams, especially with an irradiation time of 3 min, the disappearance of unfoamed region together with the well-defined cellular structure enhanced the distribution of compression stress. This helps foams to maintain stain energy storage in a reversible elastic region during load bearing in long-term compression, resulting in better recovery performance. Similar to the results of physical properties in the previous section, excessive irradiation may not be a good option for improving the elastic recovery of NRLF. The foam compression set increased, while the corresponding recoverability decreased with irradiation times of 5 and 7 min. Cell size influences elastic recovery of foam, but the detailed explanation of this relationship remains ambiguous. It has been reported that rubber foams with smaller cell diameters showed better compression set and foam recoverability owing to the thicker walls of their smaller cells [13,41]. Based on this recommendation, the foam with irradiation time of 7 min should have the highest elastic recovery due to its smallest cell size. However, we found a dissimilar result. Smaller foam cells after irradiation for 5 and 7 min had thinner walls owing to the wall thinning effect from ultrasonication. According to this observation, excessively thin cell walls are too weak to endure long-term compression stress. Hence, permanent deformation of foams with smaller cell sizes is more significant. Additionally, porosity seems to be another factor affecting the permanent compression set. Tang et al. also found that rubber foams with lower porosity were compacted and severely collapsed under long-term stress [39].

3.4. Mechanical properties

To better understand the influences of ultrasonic irradiation on the mechanical performance of NRLF, the tensile properties of NRLFs were also investigated. Fig. 8(a) presents tensile stress–strain curves of the foams at various irradiation times. All of the foams displayed identical stress–strain patterns. However, the foam with a 3 min irradiation appeared to have considerably improved tensile properties. This foam exhibited the highest ultimate tensile strength of 307.3 ± 7.1 kPa, while the other foams showed variable strengths with lower values between 225.1 ± 6.6 to 254.1 ± 3.9 kPa (Fig. 8(b)). Based on this data variability, it is difficult to study the effects of irradiation times on the tensile strength. Several researchers found that density and microscopic parameters strongly affect the mechanical strength of a foam [39,42,43]. Thus, to avoid the density effect, we calculated the specific tensile strength, which is independent of the foam density, as shown in Fig. 8 (c). Interestingly, when the density influence is excluded, the effect of irradiation time on tensile strength of NRLFs is explainable. The specific tensile strength presented a trend that initially escalated during irradiation from 0 to 3 min and afterwards decreased as irradiation was increased from 5 to 7 min. This result is reflected in the physical property data. Unfortunately, the elongation at break decreased when ultrasonication was applied. All irradiated foams showed lower elongation at break compared to the non-irradiated foam (Fig. 8(d)). The reduced elongation at break seems more apparent for the foams with irradiation times of 5 and 7 min, whose ultimate tensile strain was reduced to less than 500%.

Considering the microscopic parameters, micro-defects are well-known stress concentrations. They are readily formed when the cellular structures lack uniformity [26]. For the foams irradiated at 0 and 1 min, their microstructure uniformity appears insufficient. Micro-defects can create micro–voids at their cell walls, which further propagate to become microscopic cracks, leading to the structural fracture at
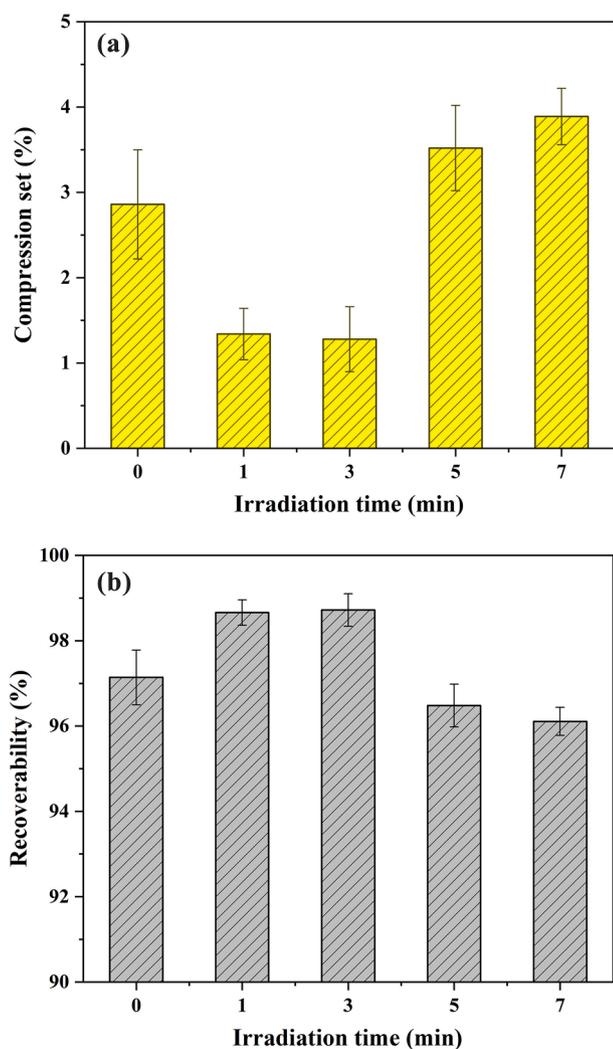
Fig. 7. Results of (a) compression set and (b) recoverability of NRLFs at various ultrasonic irradiation times.
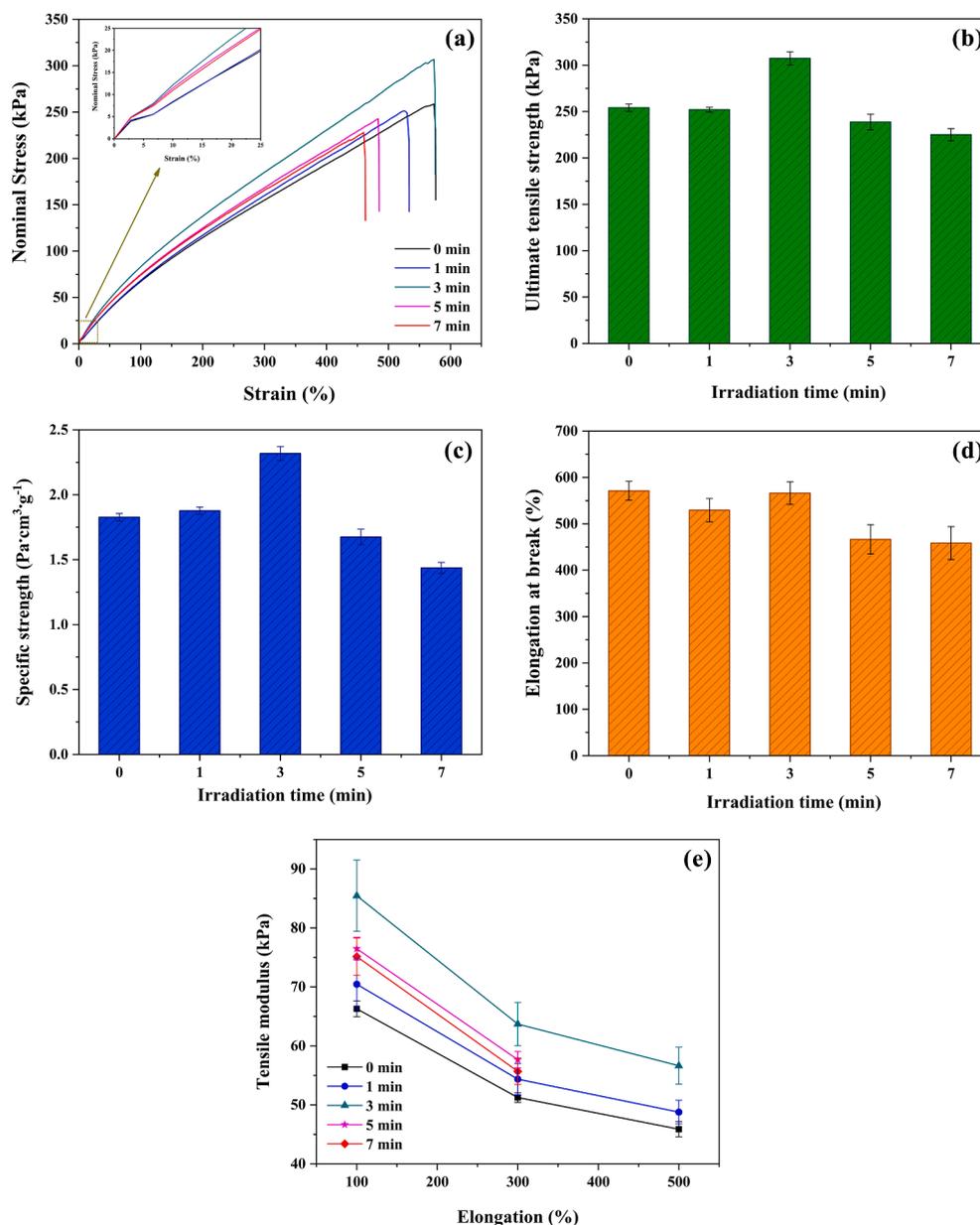
Fig. 8. Tensile properties of NRLFs as a function of ultrasonic irradiation times: (a) stress–strain curves, (b) ultimate strength, (c) specific strength, (d) elongation at break and (e) modulus.

low tensile stress. Although foams with irradiation times of 5 and 7 min have sufficient uniformity in their cellular structure, their thinner cell walls suffer from void propagation, resulting in reduced tensile strength [41]. Herein, the uniform cellular structure incorporated with moderate foam wall thickness after a 3 min irradiation time helps a foam to reach its maximum tensile strength.

The aforementioned argument, however, may not explain why the irradiated foams, which show considerably improved cell structure homogeneity, have a lower elongation at break than the foam without ultrasound treatment. Therefore, we turn our attention to the physicochemical effects of ultrasonication on molecular visualization of polymer chains. Despite there being few reports of the influence of ultrasonic irradiation on the tensile characteristics of natural rubber, it is recognized that an ultrasound field can induce chain scission in natural rubber, which reduces the chain length and molecular weight of the rubber matrix [18,44,45]. Fig. 9 proposes some possible effects of ultrasonic irradiation on natural rubber molecular chains. It can be seen that ultrasonication may acts upon rubber chains in physical (Fig. 9(a)) and

sonochemical processes (Fig. 9(b)). During initial irradiation, shear stress generated from local extreme conditions destroys non-covalent intermolecular interactions, i.e., van der Waals forces, and physical entanglements between polymer chains, leading to a disaggregation process. This process is believed to promote the ability of rubber chains to rearrange and partially pack with each other during tensile loading, resulting in strain-induced crystallization. Therefore, the tensile strength of the foams steadily increased until the irradiation time reached 3 min. With further irradiation, excessive stress causes the polymer chains to seriously distort and stretch, leading to chain breakage [18]. Apart from the physical effects, in sonochemical reactions of ultrasonic irradiation in the presence of water, both OH• and H_2O_2 are generated. These powerful oxidizing agents can possibly induce chain scission reactions of natural rubber [17,18] as presented in Fig. 9(b).

Crosslink density measurements were also conducted for vulcanized NRLFs as they can be used to confirm the effect of ultrasonication on the molecular chain scission of natural rubber [46]. These results are
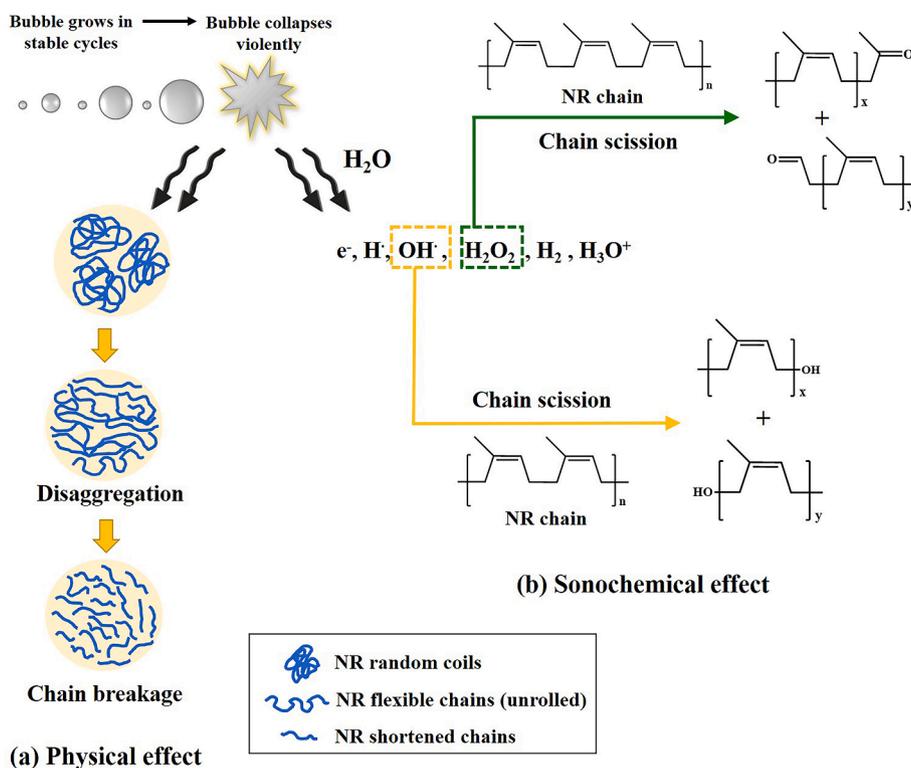
Fig. 9. Possible physicochemical effects of ultrasonic irradiation (cavitation bubble) on molecular chains of NRLF.

presented in Fig. S2. In comparison to non-irradiated foam, crosslink density values of the foams after 5 and 7 min of irradiation decreased more significantly than those of the foams with 1 and 3 min of irradiation owing to the ultrasonic activities. This affects the molecular chains of natural rubber as discussed earlier. Apart from the crosslink density results, the chemical functional groups of NRLFs were also determined using ATR-FTIR spectroscopy (Fig. S3). Significant differences were not observed among the spectra of the foam samples with various irradiation times. As a result, even though the sonochemical processes might have occurred *via* the induction of generated chemical species from ultrasonic irradiation, the predominant effect on the molecular chains of natural rubber seems to be the physical processes of ultrasonication. According to the effects of ultrasonication, the unrolled and molecularly shortened chains of irradiated foams more easily lose their chain entanglements than the compact coils of non-irradiated foam. Moreover, micro-defects are also an important factor. Microscopic cracks, which originate from the micro-defects at the cell walls, more rapidly propagate in the case of the foams with longer irradiation times due to the thinner nature of their cell walls, leading to lower elongation at break.

Even though the ultimate tensile strain of the foams decreased after applying ultrasonication, a foam with the optimum irradiation time of 3 min still maintains adequate elongation at break, 566.2 ± 24.5%, which is comparable to that of NRLFs reported in several works [47–49]. The moduli of the foams were evaluated at the elongation at break of 100, 300 and 500% (Fig. 8(e)). It was found that the moduli at 500% elongation of the foams with irradiation times of 5 and 7 min were not obtained because they broke before reaching that strain. In comparison to the non-irradiated foam, the elevated moduli for every elongation point of the irradiated foams suggest that strain-induced crystallization may occur with the help of ultrasonication. As a consequence, the strength and modulus, as well as sufficient elongation at break, suggest that formation of microcellular rubber through optimized ultrasonic-assisted processing, may improve NRLF mechanical properties.

4. Conclusions

NRLFs with improved properties have been successfully fabricated using the ultrasonic-assisted Dunlop method. Based on the experimental data, it can be summarized that microbubble implosion during ultrasonic irradiation promotes nucleation to decrease foam cell diameter, provide uniform cellular structure, and enhance cell density with increasing irradiation time. The wall thinning effect, which strongly influences the properties of the foams, also occurs with prolonging irradiation time. This is due to turbulent convection and local extreme conditions generated by the sound waves. Alternatively, the physico-mechanical properties of the foams examined by various characterization techniques indicate that only optimal irradiation time can greatly improve the foam properties. At 3 min of irradiation, several positive effects of ultrasonication can be observed. These include stable cavitation that maintains the bubble dynamics of foam nuclei promoting their stable growth and allowing them to expand without cell collapse. This results in maximal expansion and void volume fraction of the foam. As a result of changes in these foaming behaviors, the irradiated foam has the lowest foam density and indentation hardness. NRLF prepared by this optimum irradiation period also possesses well-defined microstructure with moderate cell wall thickness that enables the foam to have a negligible compression set. These could be advantageous when designing foam materials for lightweight supporting applications. Physical processes of ultrasonication appear to be the predominant effect that influences mechanical properties of the foam. Optimal irradiation may enable increased strain-induced crystallization, resulting in improved tensile performance of the foams.

CRediT authorship contribution statement

Benjatham Sukkaneewat: Conceptualization, Methodology, Investigation, Resources, Project administration, Writing – original draft, Writing – review & editing. **Songkot Utara:** Conceptualization, Methodology, Resources, Validation, Writing – review & editing.

Declaration of Competing Interest

The authors declare that they have no known competing financial interests or personal relationships that could have appeared to influence the work reported in this paper.

Acknowledgements

Appendix A. Supplementary data

Supplementary data to this article can be found online at https://doi.org/10.1016/j.ultsonch.2021.105873.

References

[1] E.-K. Lee, S.-Y. Choi, Preparation and characterization of natural rubber foams: effects of foaming temperature and carbon black content, Korean J. Chem. Eng. 24 (2007) 1070–1075.

[2] J. Martín-de León, V. Bernardo, M.Á. Rodríguez-Pérez, Nanocellular polymers: the challenge of creating cells in the nanoscale, Materials 12 (2019) 797.

[3] S. Suethao, D.U. Shah, W. Smitthipong, Recent progress in processing functionally graded polymer foams, Materials 13 (2020) 4060.

[4] Z.M. Ariff, Z. Zakaria, L.H. Tay, S.Y. Lee, Effect of foaming temperature and rubber grades on properties of natural rubber foams, J. Appl. Polym. Sci. 107 (2008) 2531–2538.

[5] D. Sridaeng, B. Sukkaneewat, N. Chueasakol, N. Chantarasiri, Copper-amine complex solution as a low-emission catalyst for flexible polyurethane foam preparation, e-Polymers 15 (2015) 119–126.

[6] A. Loykaew, S. Utara, Effect of acidic and sulfated environments on phase transformation, compressive strength and microstructure of natural rubber latex-modified cement pastes, J. Mater. Res. Technol. 9 (2020) 15496–15512.

[7] Y.-C. Wei, G.-X. Liu, L. Zhang, F. Zhao, S. Liao, M.-C. Luo, Exploring the unique characteristics of natural rubber induced by coordination interaction between proteins and Zn^{2+}, Polymer 193 (2020), 122357.

[8] D.C. Blackley, Latex foam rubber, in: Polymer Latices: Science and Technology Volume 3: Applications of latices, Springer, Netherlands, Dordrecht, 1997, pp. 229–326.

[9] N. Tangboriboon, N. Chankasem, W. Sangwan, A. Sirivat, Semi-rigid foams of calcium silicate ($CaSiO_3$) embedded in natural rubber latex, Plast. Rubber Compos. 45 (2016) 304–310.

[10] S. Sirikulchaikij, R. Kokoo, M. Khangkhamano, Natural rubber latex foam production using air microbubbles: microstructure and physical properties, Mater. Lett. 260 (2020), 126916.

[11] Z.M. Ariff, L.O. Afolabi, L.O. Salmazo, M.A. Rodriguez-Perez, Effectiveness of microwave processing approach and green blowing agents usage in foaming natural rubber, J. Mater. Res. Technol. 9 (2020) 9929–9940.

[12] L.O. Salmazo, A. Lopez-Gil, Z.M. Ariff, A.E. Job, M.A. Rodriguez-Perez, Influence of the irradiation dose in the cellular structure of natural rubber foams cross-linked by electron beam irradiation, Ind. Crops. Prod. 89 (2016) 339–349.

[13] J. Bai, X. Liao, E. Huang, Y. Luo, Q. Yang, G. Li, Control of the cell structure of microcellular silicone rubber/nanographite foam for enhanced mechanical performance, Mater. Des. 133 (2017) 288–298.

[14] H. Bayat, M. Fasihi, Curing characteristics and cellular morphology of natural rubber/silica composite foams, Polym. Bull. 77 (2020) 3171–3184.

[15] W.G.I.U. Rathnayake H. Ismail A. Baharin I.M.C.C.D. Bandara S. Rajapakse Enhancement of the antibacterial activity of natural rubber latex foam by the incorporation of zinc oxide nanoparticles J. Appl. Polym. Sci. 131 (2014) 39601.

[16] S. Phomrak, A. Nimpaiboon, B.Z. Newby, M. Phisalaphong, Natural rubber latex foam reinforced with micro- and nanofibrillated cellulose *via* Dunlop method, Polymers 12 (2020) 1959.

[17] J. Fuentes-García, J. Santoyo-Salzar, E. Rangel-Cortes, G. Goya, V. Cardozo-Mata, J. Pescador-Rojas, Effect of ultrasonic irradiation power on sonochemical synthesis of gold nanoparticles, Ultrason. Sonochem. 70 (2021), 105274.

[18] P.R. Gogate, A.L. Prajapat, Depolymerization using sonochemical reactors: a critical review, Ultrason. Sonochem. 27 (2015) 480–494.

[19] L. Redmond, R. Christianson, R. Scholl, Synthesis of polymer foam using sonic energy, in, Google Patents (2008).

[20] J.R. Youn, H. Park, Bubble growth in reaction injection molded parts foamed by ultrasonic excitation, Polym. Eng. Sci. 39 (1999) 457–468.

[21] A. Gandhi, N. Asija, H. Chauhan, N. Bhatnagar, Ultrasound-induced nucleation in microcellular polymers, J. Appl. Polym. Sci. 131 (2014) 40742.

[22] M. Yang, J. Li, Continuous ultrasound-assisted fabrication of lightweight polypropylene foam with low thermal conductivity and excellent sound insulation properties, Polym. Eng. Sci. 58 (2018) 1678–1684.

[23] G. Wang, J. Zhao, G. Wang, L.H. Mark, C.B. Park, G. Zhao, Low-density and structure-tunable microcellular PMMA foams with improved thermal-insulation and compressive mechanical properties, Eur. Polym. J. 95 (2017) 382–393.

[24] C. Torres-Sanchez, J. Corney, Effects of ultrasound on polymeric foam porosity, Ultrason. Sonochem. 15 (2008) 408–415.

[25] W. Zhai, J. Yu, J. He, Ultrasonic irradiation enhanced cell nucleation: an effective approach to microcellular foams of both high cell density and expansion ratio, Polymer 49 (2008) 2430–2434.

[26] J. Wang, W. Zhai, J. Ling, B. Shen, W. Zheng, C.B. Park, Ultrasonic irradiation enhanced cell nucleation in microcellular poly (lactic acid): a novel approach to reduce cell size distribution and increase foam expansion, Ind. Eng. Chem. Res. 50 (2011) 13840–13847.

[27] A. Gandhi, N. Bhatnagar, Significance of ultrasonic cavitation field distribution in microcellular foaming of polymers, Cell. Polym. 34 (2015) 1–14.

[28] Y. Li, Y. Song, J. Li, Y. Li, N. Li, S. Niu, A scalable ultrasonic-assisted and foaming combination method preparation polyvinyl alcohol/phytic acid polymer sponge with thermal stability and conductive capability, Ultrason. Sonochem. 42 (2018) 18–25.

[29] S. Utara, J. Klinkaewnarong, Preparation of nano-hydroxyapatite particles by ultrasonic method at 25 kHz using natural rubber latex as a templating agent, Chiang Mai J. Sci. 43 (2015) 320–328.

[30] C.S. Silva, A. Lima, S.J.F. Rodrigues, L.F.F.F. Gonçalves, Á.M. Sampaio, L. Oliveira, A. Fernandes, A.J. Pontes, Development of functionalised foam for electrostatic discharge applications, Plast. Rubber Compos. 49 (2020) 470–478.

[31] S.J. Park, S.-H. Cho, H.W. Seo, J.-D. Nam, J. Suhr, Natural cork agglomerate enabled mechanically robust rigid polyurethane foams with outstanding viscoelastic damping properties, Polymer 217 (2021), 123437.

[32] J.H. Park, S.H. Yang, H.R. Lee, C.B. Yu, S.Y. Pak, C.S. Oh, Y.J. Kang, J.R. Youn, Optimization of low frequency sound absorption by cell size control and multiscale poroacoustics modeling, J. Sound Vib. 397 (2017) 17–30.

[33] C. Torres-Sánchez, J. Corney, Identification of formation stages in a polymeric foam customised by sonication *via* electrical resistivity measurements, J. Polym. Res. 16 (2009) 461–470.

[34] J. Sundaram, B.R. Mellein, S. Mitragotri, An experimental and theoretical analysis of ultrasound-induced permeabilization of cell membranes, Biophys. J. 84 (2003) 3087–3101.

[35] G. Guo, Q. Ma, B. Zhao, D. Zhang, Ultrasound-assisted permeability improvement and acoustic characterization for solid-state fabricated PLA foams, Ultrason. Sonochem. 20 (2013) 137–143.

[36] F.F. Adam, R.A. Istiqomah, M.A. Budianto, P.N. Trisanti, S. Sumarno, Study of microcellular foaming of polystyrene aided with 45 kHz of ultrasound waves energy, Polym. Plast. Technol. Mater. 59 (2020) 1343–1349.

[37] L.O. Salmazo, A. Lopéz-Gil, Z.M. Ariff, M.L. Rodriguez-Mendez, A.E. Job, M. A. Rodriguez-Perez, Study of the foaming kinetics in epoxidized natural rubber foams crosslinked by electron beam irradiation, Macromol. Chem. Phys. 219 (2018) 1800295.

[38] E.A. Flores-Johnson, Q.M. Li, Indentation into polymeric foams, Int. J. Solids Struct. 47 (2010) 1987–1995.

[39] W. Tang, X. Liao, Y. Zhang, J. Li, G. Wang, G. Li, Mechanical–microstructure relationship and cellular failure mechanism of silicone rubber foam by the cell microstructure designed in supercritical CO_2, J. Phys. Chem. C 123 (2019) 26947–26956.

[40] K.W. Park, G.H. Kim, S.R. Chowdhury, Improvement of compression set property of ethylene vinyl acetate copolymer/ethylene-1-butene copolymer/organoclay nanocomposite foams, Polym. Eng. Sci. 48 (2008) 1183–1190.

[41] S. Kiatkamjornwong, P. Thinakorn, P. Tasakorn, Foaming conditions of high density polyethylene–natural rubber blends, Plast. Rubber Compos. 29 (2000) 177–186.

[42] J. Lederman, The prediction of the tensile properties of flexible foams, J. Appl. Polym. Sci. 15 (1971) 693–703.

[43] J.-B. Bao, A.N. Junior, G.-S. Weng, J. Wang, Y.-W. Fang, G.-H. Hu, Tensile and impact properties of microcellular isotactic polypropylene (PP) foams obtained by supercritical carbon dioxide, J. Supercrit. Fluids. 111 (2016) 63–73.

[44] A. Fainleib, R.V. Pires, E.F. Lucas, B.G. Soares, Degradation of non-vulcanized natural rubber-renewable resource for fine chemicals used in polymer synthesis, Polímeros 23 (2013) 441–450.

[45] S. Utara, U. Moonart, Effects of frequency and sonication time on ultrasonic degradation of natural rubber latex, Adv. Mater. Res. 747 (2013) 721–724.

[46] X. Sun, A.I. Isayev, Ultrasound devulcanization: comparison of synthetic isoprene and natural rubbers, J. Mater. Sci. 42 (2007) 7520–7529.

[47] S.N.I. Kudori, H. Ismail, S.R. Khimi, Tensile and morphological properties on kenaf core or bast filled natural rubber latex foam (NRLF), Mater. Today: Proc. 17 (2019) 609–615.

[48] S.N.I. Kudori, H. Ismail, The effects of filler contents and particle sizes on properties of green kenaf-filled natural rubber latex foam, Cell. Polym. 39 (2020) 57–68.

[49] A.S.M. Bashir, Y. Manusamy, T.L. Chew, H. Ismail, S. Ramasamy, Mechanical, thermal, and morphological properties of (eggshell powder)-filled natural rubber latex foam, J. Vinyl Addit. Technol. 23 (2017) 3–12.